# Magnetic resonance in a singlet-triplet Josephson junction

Lars Elster,* Manuel Houzet, and Julia S. Meyer
*Univ. Grenoble Alpes, INAC-PHELIQS, F-38000 Grenoble, France*
*and CEA, INAC-PHELIQS, F-38000 Grenoble, France*

(Received 2 September 2015; revised manuscript received 19 February 2016; published 16 March 2016)

We study a singlet-triplet Josephson junction between a conventional $s$-wave superconductor and an unconventional $p_x$-wave superconductor. The Andreev spectrum of the junction yields a spontaneous magnetization in equilibrium. This allows manipulating the occupation of the Andreev levels using an ac Zeeman field. The induced Rabi oscillations manifest themselves as a resonance in the current-phase relation. For a circularly polarized magnetic field, we find a spin selection rule, yielding Rabi oscillations only in a certain interval of the superconducting phase difference.

DOI: 10.1103/PhysRevB.93.104519

## I. INTRODUCTION

The current-phase relation of a Josephson junction contains information about the Andreev levels and their occupations. Junctions formed between unconventional superconductors have exotic bound states leading to unusual current-phase relations. Among unconventional Josephson junctions, those realized between singlet and triplet superconductors are of special interest, because of their incompatible spin pairing symmetries. Their equilibrium properties have been studied for various types of heterogeneous junctions [1–7].

For instance, a Josephson junction between a conventional spin-singlet, $s$-wave superconductor and an unconventional spin-triplet, $p_x$-wave superconductor displays exotic spin properties. Namely, it hosts two spin-polarized Andreev bound states, which have the same spin [8]. In equilibrium, this results in a spontaneous magnetization that is $2\pi$ periodic in the superconducting phase difference. On the other hand, a $\pi$-periodic equilibrium supercurrent, which does not probe the exotic spin properties, is found [9–11]. The spin properties of the Andreev levels open the possibility for spin manipulation, using a time-dependent Zeeman field. A similar idea, the manipulation of the Andreev levels in spin active Josephson junctions between conventional superconductors, has already been reported [12].

In this article, we show that an ac Zeeman field leads to coherent Rabi oscillations between different spin states of the singlet-triplet junction. These Rabi oscillations manifest themselves as resonances in the current-phase relation. For a circularly polarized magnetic field, we find a spin selection rule, yielding Rabi oscillations only in a certain interval of the superconducting phase difference. The Zeeman field also induces incoherent transitions between the bound states and the continuum states. In principle, these transitions, which we treat within a master equation approach, could give rise to a decay mechanism for the Rabi oscillations. However, we find that, due to spin and energy constraints, these processes do not coexist with the Rabi oscillations.

Resonances due to Rabi oscillations between Andreev levels were predicted in the current-phase relation of superconducting atomic contacts subject to an ac phase [13,14]. Following Ref. [12], resonances due to an ac magnetic field may be expected in spin-active Josephson junctions, provided their ground state is magnetic. This was not achieved in a model that considered a Josephson junction through a precessing spin [15] and, indeed, no resonance was detected in that work. By contrast, the ground state magnetization of singlet-triplet junctions is robust and allows for resonances without any fine tuning.

A possible experimental realization of our proposal could be based on the $(TMTSF)_2X$ Bechgaard salts [16], as suggested in Ref. [8]. Alternatively, we propose to realize a junction between conventional superconductors separated by a ferromagnetic semiconducting nanowire, as illustrated in Fig. 1(b). The gate would allow for the realization of a barrier with tunable transparency. Furthermore, an effective $p_x$-wave superconductor is realized when the length of the nanowire between the gate and one of the leads matches the coherence length $\xi_F$ for the superconducting correlations induced in the nanowire.

This article is organized in the following way. In Sec. II we introduce the model we use to describe a singlet-triplet junction in the presence of a Zeeman field. In Sec. III, we discuss the different field-induced processes and their spin and energy constraints. The dynamics of the Andreev bound states is developed in Sec. IV, including the calculation of the transition rates. In Sec. V, we show the current-phase relation of the junction for a circularly and a linearly polarized magnetic field. Finally we conclude in Sec. VI. Technical details are given in the appendices.

## II. MODEL

The Hamiltonian describing a Josephson junction between an $s$-wave superconductor and a one-dimensional, time-reversal symmetric $p_x$-wave superconductor reads

$$H = \int dx\, \Psi^\dagger \mathcal{H} \Psi, \tag{1}$$

where $\Psi = (R_\downarrow, L_\uparrow^\dagger, L_\downarrow, R_\uparrow^\dagger)^T$, and $R_\sigma^\dagger$ and $L_\sigma^\dagger$ are creation operators for right-moving (R) and left-moving (L) electrons with spin $\sigma = \uparrow, \downarrow$, respectively. The Bogoliubov–de Gennes

*lars.elster@cea.fr

 

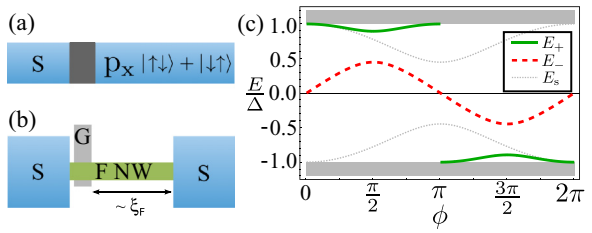


FIG. 1. (a) Model of a Josephson junction between an $s$-wave and a $p_x$-wave superconductor. (b) Setup of an effective singlet/triplet junction using a semiconducting ferromagnetic nanowire (F NW) contacted with conventional singlet superconductors (S). The gate (G) allows for realizing a barrier with tunable transparency. (c) Energy-phase relation of the two bound states for the transmission $T = 0.8$ (thick lines). The continuum of states is indicated in gray. All states shown have spin $\downarrow$. The bound state energies for a junction between two $s$-wave superconductors are given for comparison (thin lines).

Hamiltonian $\mathcal{H}$ is given as

$$\mathcal{H} = v_F p \eta_z \tau_z + U(x)\eta_x\tau_z - \Delta_s(x)\tau_x + \Delta_p(x)\eta_z\tau_x e^{-i\tau_z\phi}, \tag{2}$$

where $\tau_{x,y,z}$ and $\eta_{x,y,z}$ denote Pauli matrices in particle-hole and R/L spaces, respectively. The first term in Eq. (2), with Fermi velocity $v_F$ and momentum operator $p$, is the kinetic energy. The second term describes a scalar potential $U(x)$ in the central region of the junction, $0 < x < L$, where $L$ is the junction length. It gives rise to an electronic transmission probability $T$, when the junction is in the normal state. The third term describes $s$-wave pairing with gap $\Delta_s(x) = \Delta_s\theta(-x)$, where $\theta$ is the Heaviside step function, in the left lead. The last term describes $p_x$-wave pairing with gap $\Delta_p(x) = \Delta_p\theta(x - L)$ between electrons having opposite spins along the $z$ direction in the right lead. That is, the spin quantization axis is chosen along the **d** vector [17] of the triplet pair potential. For simplicity, we will restrict our analysis to the case $\Delta_s = \Delta_p \equiv \Delta$.[1] The superconducting phase difference across the junction is denoted $\phi$. Note that we use units where $\hbar = 1$.

In the short-junction limit, $L \ll v_F/\Delta$, the Hamiltonian (2) allows for two bound states with energies [8]

$$E_\pm = \frac{\mathrm{sgn}(\sin\phi)}{\sqrt{2}}\Delta\sqrt{1 \pm \sqrt{1 - T^2\sin^2\phi}}, \tag{3}$$

and wave functions $\psi_\pm(x)$ given in Appendix A. Note that the choice of the spinor $\Psi$ implies that we are considering states with spin down only. Furthermore, Eq. (2) allows for a fourfold degenerate continuum of (outgoing) propagating states with energies $E$ ($|E| > \Delta$) and wave functions $\psi_{E\mu}(x)$, where $\mu$ is a degeneracy index. Using a Bogoliubov transformation,

$$\Psi(x) = \sum_{\nu=\pm}\psi_\nu(x)\gamma_\nu + \sum_{E,\mu}\psi_{E\mu}(x)\gamma_{E\mu}, \tag{4}$$

where $\gamma_\nu$ and $\gamma_{E\mu}$ are annihilation operators for quasiparticles in the bound state with energy $E_\nu$ and for quasiparticles in the continuum with energy $E$ and degeneracy index $\mu$, respectively, we may diagonalize (1) to obtain

$$H = \sum_{\nu=\pm} E_\nu\gamma_\nu^\dagger\gamma_\nu + \sum_{E,\mu} E\gamma_{E\mu}^\dagger\gamma_{E\mu}. \tag{5}$$

A typical spectrum is shown in Fig. 1(c). Note that at vanishing coupling, $T \to 0$, the spectrum of the $s$-wave lead is gapped, while the $p_x$-wave lead, which realizes two copies of the Kitaev model [18] in opposite spin sectors, allows for a zero-energy edge state. A finite coupling moves this state to finite energy and yields the bound state $\nu = -$ [7], while a second bound state ($\nu = +$) detaches from the continuum. In contrast to conventional junctions, both bound states carry the same spin ($\sigma = \downarrow$).

The bound state occupations, $n_\nu = \langle\gamma_\nu^\dagger\gamma_\nu\rangle$, determine the magnetization carried by the junction, $M = -(\mu_B/4)\sum_{\nu=\pm}(2n_\nu - 1)$, where $\mu_B$ is the Bohr magneton. In equilibrium, $n_\nu = f(E_\nu)$, where $f$ is the Fermi function. As a result, the junction carries a spontaneous magnetization, which is $2\pi$ periodic in the phase difference [8].

The Josephson current is given as

$$I = 2e\sum_{\nu=\pm}\frac{dE_\nu}{d\phi}\left(n_\nu - \frac{1}{2}\right). \tag{6}$$

The equilibrium supercurrent is spin insensitive and, therefore, $\pi$ periodic.

Thus, to probe the peculiar spin properties of the junction, we have to consider out-of-equilibrium effects. In order to manipulate the bound state occupations, we apply a weak ac magnetic field, described by the Zeeman Hamiltonian

$$H_Z = \mu_B\sum_{s,s'=\uparrow,\downarrow}\int dx\, \boldsymbol{B}\cdot(R_s^\dagger\boldsymbol{\sigma}_{ss'}R_{s'} + L_s^\dagger\boldsymbol{\sigma}_{ss'}L_{s'}). \tag{7}$$

We consider two different polarizations for the magnetic field $\boldsymbol{B}$. First, let us consider a circularly polarized field $\boldsymbol{B} = B(\cos\Omega t, \sin\Omega t, 0)$, where $\Omega$ is the driving frequency. Such a circularly polarized field, perpendicular to the **d** vector of the triplet pair potential, leads to spin-flip processes: The spin of the system changes by $\Delta S_z = \mathrm{sgn}(\Omega)$ when a photon is absorbed, whereas it changes by $\Delta S_z = -\mathrm{sgn}(\Omega)$ when a photon is emitted. Second, we investigate a linearly polarized field $\boldsymbol{B} = 2B(\cos\Omega t, 0, 0)$. Such a field can be viewed as the superposition of two circularly polarized fields with opposite helicities. Therefore, we concentrate our discussion on the case of circular polarization and comment afterwards on the linear polarization.

In order to identify the field-induced processes, we express Eq. (7) in terms of the quasiparticle operators using the Bogoliubov transformation (4). We find

$$H_Z = \mu_B B e^{-i\Omega t}\left(V_{+,-}\gamma_+\gamma_- + \sum_{E;\mu,\nu}V_{\nu,E\mu}\gamma_\nu\gamma_{E\mu} + \frac{1}{2}\sum_{E,E';\mu,\mu'}V_{E\mu,E'\mu'}\gamma_{E\mu}\gamma_{E'\mu'}\right) + \mathrm{H.c.}, \tag{8}$$

where $V_{\lambda,\lambda'} = \int dx\, \psi_\lambda^T\eta_x(-i\tau_y)\psi_{\lambda'}$ for $\lambda,\lambda' \in \{+, -, E\mu\}$.

[1] When $\Delta_s \neq \Delta_p$, our conclusions remain valid in the regime of superconducting phase difference where two Andreev bound states exist, cf. Ref. [8].

Thus the field couples two quasiparticle states. According to Eq. (8), three different types of processes are possible: transitions involving only bound states (first term), transitions involving a bound state and a continuum state (second term), and transitions involving only continuum states (third term).

## III. DISCUSSION

In this section we discuss the different processes described by Eq. (8) and give the constraints in spin and energy, that they are subjected to.

Let us start with a circularly polarized magnetic field. For definiteness, we consider the case $\Omega < 0$. For the discussion of the spin properties, we note that the destruction of a quasiparticle with spin down at negative energies corresponds to the creation of a quasiparticle with spin up at positive energies. So far, we used both positive and negative energies for spin $\downarrow$. In the following, we will work with both spin directions, but only positive quasiparticle energies. Furthermore, we assume that the temperature is low, such that the continuum states are empty.

The transitions involving only bound states correspond to Rabi oscillations, i.e., coherent oscillations between the state $|0\rangle$, where both bound states are empty, and the state $|2\rangle$, where both bound states are occupied. They occur when the oscillation frequency $|\Omega|$ matches the Rabi frequency, $\Omega_R = |E_+(\phi) + E_-(\phi)|$. Using the energy dispersions given by Eq. (3), the interesting frequency regime is, thus, given by $\Delta < |\Omega| < \sqrt{2}\Delta$.[2] Then, sweeping the phase at fixed frequency, the resonance condition is met for four different values of the phase: $\phi_0$, $\pi - \phi_0$, $\pi + \phi_0$, and $2\pi - \phi_0$. However, the spin selection rule imposes a further constraint. Namely, at $\Omega < 0$, Rabi oscillations are possible only if the bound states carry a spin down, which is the case in the interval $0 < \phi < \pi$. Thus, the circularly polarized field leads to Rabi oscillations only at two values of the phase: $\phi_0$ and $\pi - \phi_0$.

Transitions involving a bound and a continuum state change the parity of the bound state occupation, connecting the even-parity subspace $\{|0\rangle, |2\rangle\}$ to the odd-parity subspace $\{|-\rangle, |+\rangle\}$, where $|\nu\rangle$ denotes the state in which only the bound state with energy $|E_\nu|$ is occupied. [For a sketch of the four states of the junction, see Fig. 2(a).] This would represent a decay mechanism for the Rabi oscillations. We may distinguish two different processes, sketched in Fig. 2(b).

In an *ionization* process, a quasiparticle from a bound state is promoted to a continuum state. Energy conservation imposes $|\Omega| > \Delta - |E_\nu|$ for such a process. In the frequency range of interest for Rabi oscillations, this condition is always met. However, the spin selection rule imposes that, at $\Omega < 0$, the bound state carries a spin up, which is the case in the interval $\pi < \phi < 2\pi$ only. Thus, Rabi oscillations and ionization processes occur in different phase intervals.

In a *refill* process, a Cooper pair is broken such that one quasiparticle occupies a bound state, whereas the second quasiparticle is promoted to a continuum state. Here energy conservation imposes $|\Omega| > \Delta + |E_\nu|$. In the frequency range

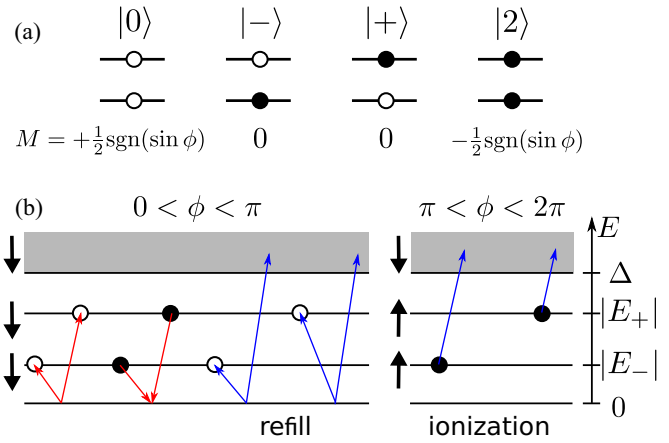


FIG. 2. (a) Possible states of the junction and their magnetization $M$. Full (open) dots represent occupied (empty) states. (b) Transitions induced by a circularly polarized magnetic field with $\Omega < 0$. The shaded region is the continuum of states. The thick black arrows denote the spin of the states. Absorption (emission) of a photon changes the spin by $\Delta S_z = -1$ ($\Delta S_z = +1$).

of interest for Rabi oscillations, this condition is never met for the state with energy $|E_+|$. By contrast, for the state with energy $|E_-|$, one obtains a critical phase $\phi_c$ such that the condition is met in the phase intervals $[-\phi_c, \phi_c]$ and $[\pi - \phi_c, \pi + \phi_c]$. We find $\phi_c < \phi_0$. Thus, Rabi oscillations and refill processes also occur in different phase intervals. Note that, here, the spin selection rule imposes that, at $\Omega < 0$, the bound state carries a spin down, which is the case in the interval $0 < \phi < \pi$.

We conclude that the field-induced transitions do not provide a decay mechanism for the Rabi oscillations due to energy and spin constraints. However, such a decay may be due to other parity nonconserving processes related to, e.g., quantum phase fluctuations due to the resistive environment of the junction [19,20].

Finally, transitions involving only continuum states have a threshold $|\Omega| > 2\Delta$. Thus, they do not play a role in the frequency range of interest for Rabi oscillations.

Let us now consider a linearly polarized magnetic field. As already mentioned, this field can be viewed as the superposition of two circularly polarized fields with opposite helicities. Thus, the spin selection rule is always met by one of the helicities and there is no spin constraint anymore. As a consequence, Rabi oscillations may now occur at the four phases $\phi_0$, $\pi - \phi_0$, $\pi + \phi_0$, and $2\pi - \phi_0$. Furthermore, the field-induced ionization rates are non-zero for all superconducting phase differences. Due to energy constraints, the refill process of the state with energy $|E_-|$ exists only in the phase intervals $[-\phi_c, \phi_c]$ and $[\pi - \phi_c, \pi + \phi_c]$.

## IV. ANDREEV BOUND STATES DYNAMICS

The modifications of the bound state occupations induced by the different processes discussed in Sec. III may lead to strong deviations of the Josephson current (6) from its equilibrium value. To compute the steady-state Josephson

[2]Note that as $T$ decreases the maximal value of $|E_+(\phi) + E_-(\phi)|$ decreases from its maximum $\sqrt{2}\Delta$ at $T = 1$ to $\Delta$ at $T = 0$.

current, we introduce the matrix elements $\rho_{\alpha\beta} = \langle\alpha|\rho|\beta\rangle$ of the reduced density matrix $\rho$, where $|\alpha\rangle, |\beta\rangle \in \{|0\rangle, |+\rangle, |-\rangle, |2\rangle\}$, so that Eq. (6) reads

$$I = (I_+ + I_-)(\rho_{00} - \rho_{22}) + (I_+ - I_-)(\rho_{--} - \rho_{++}) \tag{9}$$

with $I_\pm = -e(d|E_\pm|/d\phi)$.[3]

To evaluate the current, we introduce a standard master equation in the Born-Markov approximation to determine the steady-state occupations $\rho_{\alpha\alpha}$. We also compute the field-induced transition rates involving continuum states.

### A. Master equation approach

The time evolution of the density matrix entries for a circularly polarized field is given by

$$\frac{d}{dt}\begin{pmatrix}\rho_{00}\\ \rho_{22}\\ \bar\rho_{02}\\ \bar\rho_{20}\\ \rho_{--}\\ \rho_{++}\end{pmatrix} = \begin{pmatrix} -\Gamma^{\rm R}_- - \Gamma^{\rm R}_+ & 0 & i\frac{\omega_1^*}{2} & -i\frac{\omega_1}{2} & \Gamma^{\rm I}_- & \Gamma^{\rm I}_+ \\ 0 & -\Gamma^{\rm I}_- - \Gamma^{\rm I}_+ & -i\frac{\omega_1^*}{2} & i\frac{\omega_1}{2} & \Gamma^{\rm R}_+ & \Gamma^{\rm R}_- \\ i\frac{\omega_1}{2} & -i\frac{\omega_1}{2} & i\delta\omega - \frac{\Gamma_\Sigma}{2} & 0 & 0 & 0 \\ -i\frac{\omega_1^*}{2} & i\frac{\omega_1^*}{2} & 0 & -i\delta\omega - \frac{\Gamma_\Sigma}{2} & 0 & 0 \\ \Gamma^{\rm R}_- & \Gamma^{\rm I}_+ & 0 & 0 & -\Gamma^{\rm I}_- - \Gamma^{\rm R}_+ & 0 \\ \Gamma^{\rm R}_+ & \Gamma^{\rm I}_- & 0 & 0 & 0 & -\Gamma^{\rm R}_- - \Gamma^{\rm I}_+ \end{pmatrix}\begin{pmatrix}\rho_{00}\\ \rho_{22}\\ \bar\rho_{02}\\ \bar\rho_{20}\\ \rho_{--}\\ \rho_{++}\end{pmatrix}. \tag{10}$$

Here, $\bar\rho_{02} = e^{i\Omega t}\rho_{02}$ and $\bar\rho_{20} = e^{-i\Omega t}\rho_{20}$ are the coherences in the even sector and $\omega_1 = 2V_{+,-} - \mu_{\rm B}B$ with $|V_{+,-}|^2 = T^2|\sin\phi|(1 + |\sin\phi|)/(1 + T|\sin\phi|)^2$. Further, $\Gamma^{\rm I/R}_\nu$ are the ionization (I) and refill (R) rates of the state $\nu$, respectively. The other ten elements of the $4 \times 4$ density matrix that are not shown remain zero along the time evolution.

The stationary occupations are obtained from the master equation, Eq. (10), by setting $\dot\rho = 0$. They are most conveniently expressed in the form

$$\rho^{\rm st}_{\alpha\alpha} = \rho^\infty_{\alpha\alpha} + \frac{\Gamma^2}{\Gamma^2 + (2\delta\omega)^2}(\rho^0_{\alpha\alpha} - \rho^\infty_{\alpha\alpha}). \tag{11}$$

The occupations far from resonance ($\rho^\infty_{\alpha\alpha}$) are given as

$$\rho^\infty_{00} = \frac{\Gamma^{\rm I}_+\Gamma^{\rm I}_-}{\Gamma_+\Gamma_-}, \quad \rho^\infty_{--} = \frac{\Gamma^{\rm I}_+\Gamma^{\rm R}_-}{\Gamma_+\Gamma_-}, \quad \rho^\infty_{++} = \frac{\Gamma^{\rm I}_-\Gamma^{\rm R}_+}{\Gamma_+\Gamma_-}, \quad \rho^\infty_{22} = \frac{\Gamma^{\rm R}_+\Gamma^{\rm R}_-}{\Gamma_+\Gamma_-}, \tag{12}$$

whereas the occupations at the resonance ($\rho^0_{\alpha\alpha}$) take the form

$$\rho^0_{00} = \rho^\infty_{00}\left\{1 + \frac{|\omega_1|^2}{\Gamma^2}\left[\left(1 + \frac{\Gamma^{\rm R}_-}{\Gamma^{\rm I}_+}\right)\left(1 + \frac{\Gamma^{\rm R}_+}{\Gamma^{\rm I}_-}\right) - \frac{\Gamma^2_\Sigma}{\Gamma_+\Gamma_-}\right]\right\}, \tag{13}$$

$$\rho^0_{--} = \rho^\infty_{--}\left\{1 + \frac{|\omega_1|^2}{\Gamma^2}\left[\frac{(\Gamma^{\rm I}_+ + \Gamma^{\rm R}_-)^2}{\Gamma^{\rm I}_+\Gamma^{\rm R}_-} - \frac{\Gamma^2_\Sigma}{\Gamma_+\Gamma_-}\right]\right\}, \tag{14}$$

$$\rho^0_{++} = \rho^\infty_{++}\left\{1 + \frac{|\omega_1|^2}{\Gamma^2}\left[\frac{(\Gamma^{\rm I}_- + \Gamma^{\rm R}_+)^2}{\Gamma^{\rm I}_-\Gamma^{\rm R}_+} - \frac{\Gamma^2_\Sigma}{\Gamma_+\Gamma_-}\right]\right\}, \tag{15}$$

$$\rho^0_{22} = \rho^\infty_{22}\left\{1 + \frac{|\omega_1|^2}{\Gamma^2}\left[\left(1 + \frac{\Gamma^{\rm I}_+}{\Gamma^{\rm R}_-}\right)\left(1 + \frac{\Gamma^{\rm I}_-}{\Gamma^{\rm R}_+}\right) - \frac{\Gamma^2_\Sigma}{\Gamma_+\Gamma_-}\right]\right\}. \tag{16}$$

For the linear polarization, we introduce a rotating-wave approximation to describe the vicinity of the Rabi resonances. Under the assumption $\Gamma \ll \Delta$, we find that the rates for a linearly polarized field are given by the sum of the rates for a circular field with positive and negative helicity, i.e., $\Gamma^{\rm X}_\nu = \Gamma^{\rm X}_\nu(\Omega) + \Gamma^{\rm X}_\nu(-\Omega)$, where X = I,R. With this substitution, the expressions for the occupations given above remain valid for the linearly polarized field.

As pointed out in Sec. III, all field-induced decay rates are zero in the phase interval $[\phi_{\rm c}, \pi - \phi_{\rm c}]$. Therefore, we introduce phenomenological rates $\gamma$ to describe the parity nonconserving processes due to the environment. At low temperature, the refill processes are negligible,[4] and we are left with two rates $\gamma^{\rm I}_\nu$. The total rate for each process is given by the sum of the field-induced rate and the phenomenological rate.

### B. Transition rates

The field-induced transition rates for the ionization and refill processes involving the bound state $\nu$ can be calculated from Eq. (8) using Fermi's golden rule,

$$\Gamma^{\rm I/R}_\nu(\Omega) = 2\pi(\mu_{\rm B}B)^2\int_\Delta^\infty dE\,\rho(E)\sum_\mu |V_{\nu,\mp E\,\mathrm{sgn}(\sin\phi)\mu}|^2 \times \delta[\Omega + (|E_\nu| \mp E)\,\mathrm{sgn}(\sin\phi)]. \tag{17}$$

Here $\rho(E) = (2\pi v_{\rm F})^{-1}E/\sqrt{E^2 - \Delta^2}$ is the density of states in the leads. The rates $\Gamma^{\rm I/R}_\nu$, whose typical amplitude is $\sim (\mu_{\rm B}B)^2/\Delta$, vanish below the threshold frequency $\Omega^{\rm I/R}_{\nu,{\rm c}} = \Delta \mp |E_\nu|$, as discussed above. Furthermore, they are suppressed at large frequencies $|\Omega| \gg \Delta$, while they display a maximum in

[3] Equation (9) neglects a small modification of the current expectation values $I_\pm$ [of order $\mathcal{O}(\mu_{\rm B}^2B^2/\Delta^2)$], while it accounts for a large effect [of order $\mathcal{O}(1)$] due to modified Andreev occupations. It also neglects charge-imbalance related effects in the presence of ac drive [20] with the standard assumption of fast inelastic relaxation in the leads.

[4] Such a process would require either an excess quasiparticle above the gap or a spin-flip process.

the vicinity of the threshold frequency. In general, Eq. (17) can be evaluated numerically. As an example, Fig. 3 shows plots of the different rates as a function of the driving frequency for a transmission of $T = 0.8$. Analytical expressions for Eq. (17) can also be obtained in the limit of a transparent junction ($T = 1$) and for a tunnel junction ($T \ll 1$) (see Appendix B for details).

### 1. Transparent junction

For a transparent junction, we find

$$\Gamma_\nu^{\mathrm{I/R}} = \frac{(\mu_B B)^2}{\Delta} \frac{4|\epsilon_{\bar\nu}|\sqrt{(|\tilde\Omega| \pm |\epsilon_\nu|)^2 - 1}[|\tilde\Omega| \pm |\epsilon_\nu| + \mathrm{sgn}\,(\Omega)|\epsilon_{\bar\nu}| \sin\phi]}{|\tilde\Omega|^2(|\tilde\Omega| \pm 2|\epsilon_\nu|)^2[(|\tilde\Omega| \pm |\epsilon_\nu|)^2 - |\epsilon_{\bar\nu}|^2]}, \tag{18}$$

where we defined $\tilde\Omega = \Omega/\Delta$ and $\epsilon_\nu = E/\Delta$, where $E_\nu$ is given in Eq. (3).

Near the threshold frequency, $\tilde\Omega_{\nu,\mathrm{c}}^{\mathrm{I/R}} = 1 \mp |\epsilon_\nu|$, the rates $\Gamma_\nu^{\mathrm{I/R}}$ grow as $\sqrt{\delta\tilde\Omega}$, where $\delta\tilde\Omega = |\tilde\Omega| - \tilde\Omega_{\nu,\mathrm{c}}^{\mathrm{I/R}}$. At large frequencies they decrease as $1/\tilde\Omega^4$. In order to describe the rates around their maximum, where the crossover between the two scaling behaviours takes place, we concentrate on the regime $\phi, \delta\tilde\Omega \ll 1$ (a similar situation occurs for phases $\phi$ close to $\pi$). We obtain

$$\Gamma_-^{\mathrm{I/R}} = \frac{(\mu_B B)^2}{\Delta} \frac{2\sqrt{2}\sqrt{\delta\tilde\Omega}}{\delta\tilde\Omega + \frac{\phi^2}{8}} \quad \text{and}$$
$$\Gamma_+^{\mathrm{I/R}} = \frac{(\mu_B B)^2}{\Delta} \frac{\sqrt{\delta\tilde\Omega}\,\phi}{\sqrt{2}\left(\delta\tilde\Omega + \frac{\phi^2}{8}\right)^2}. \tag{19}$$

Thus we find that the former reaches its maximum, $\Gamma_{-,\max}/[(\mu_B B)^2/\Delta] = 4/\phi$, at $\delta\tilde\Omega_{-,\max} = \phi^2/8$, while the later reaches its maximum, $\Gamma_{+,\max}/[(\mu_B B)^2/\Delta] = 6\sqrt{3}/\phi^2$, at $\delta\tilde\Omega_{+,\max} = \phi^2/24$.

At larger $\phi$, the maximum is less pronounced and further away from the threshold than for small $\phi$. Note that, for $\phi = \pi/2$, $\Gamma_+^{\mathrm{I/R}} = \Gamma_-^{\mathrm{I/R}}$, since the bound states are degenerate.

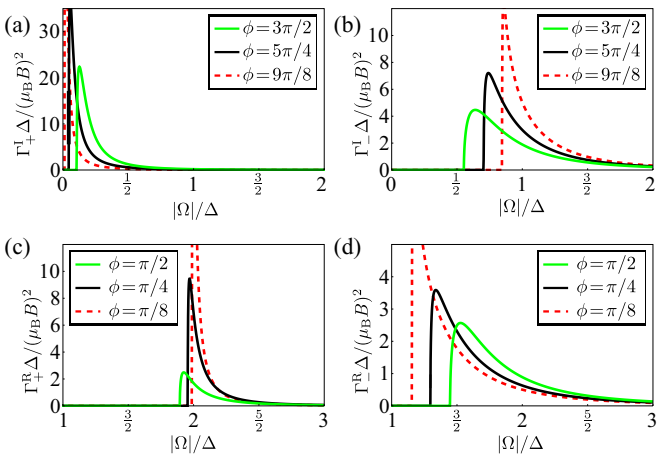


FIG. 3. Field-induced ionization (I) and refill (R) rates for $T = 0.8$ as a function of the driving frequency $\Omega < 0$ for several phase differences $\phi$. (a) Ionization rate of the state $\nu = +$. (b) Ionization rate of the state $\nu = -$. (c) Refill rate of the state $\nu = +$. (d) Refill rate of the state $\nu = -$.

### 2. Tunnel junction

For an opaque junction ($T = 0$) only the bound state $\nu = -$ exists, and

$$\Gamma_-^{\mathrm{I/R}} = \frac{(\mu_B B)^2}{\Delta} \frac{16\sqrt{|\tilde\Omega|^2 - 1}}{|\tilde\Omega|^5}. \tag{20}$$

Since the bound state energy is zero, the rate is identical for refill and ionization processes. Near the threshold frequency, $\tilde\Omega_{\mathrm{c}} = 1$, the rate grows as $\sqrt{\delta\tilde\Omega}$. It reaches its maximum, $\Gamma_{\max}/[(\mu_B B)^2/\Delta] = 2^8/(25\sqrt{5})$, at $|\tilde\Omega_{\max}| = \sqrt{5}/2$ and decreases as $1/\tilde\Omega^4$ at large frequencies. Note, that the rate does not depend on the superconducting phase difference, since the bound state energy is independent of the phase.

At small but finite transparency, an additional peak structure develops near the threshold frequency for ionization/refill processes, $\tilde\Omega_{\nu,\mathrm{c}}^{\mathrm{I/R}} = 1 \mp |\epsilon_\nu|$. For $\delta\tilde\Omega = |\tilde\Omega| - \tilde\Omega_{\nu,\mathrm{c}}^{\mathrm{I/R}} \ll 1$ the rates for the $\nu = -$ state take the form

$$\Gamma_-^{\mathrm{I/R}} = \frac{(\mu_B B)^2}{\Delta}\left[f^{\mathrm{I/R}}\left(\frac{\delta\tilde\Omega}{T^2}\right) + T g^{\mathrm{I/R}}\left(\frac{\delta\tilde\Omega}{T^2}\right)\right], \tag{21}$$

where

$$f^{\mathrm{I/R}}(x) = \frac{1}{\sqrt{2x}} \frac{32x(1 \mp |\sin\phi|)}{8x + \sin^2\phi}$$
$$\approx \begin{cases} 16\sqrt{2x}\,\frac{1\mp|\sin\phi|}{\sin^2\phi} & \text{for } x \ll 1, \\ 2\sqrt{\frac{2}{x}}(1 \mp |\sin\phi|) & \text{for } x \gg 1, \end{cases} \tag{22}$$

$$g^{\mathrm{I/R}}(x) = \frac{1}{\sqrt{2x}} \frac{16x(16x + 1 \pm |\sin\phi|)}{8x + \sin^2\phi}$$
$$\approx \begin{cases} 8\sqrt{2x}\,\frac{1\pm|\sin\phi|}{\sin^2\phi} & \text{for } x \ll 1, \\ 16\sqrt{2x} & \text{for } x \gg 1. \end{cases} \tag{23}$$

The first term describes a narrow peak of height $(\mu_B B)^2/\Delta$ near $\delta\tilde\Omega \sim T^2$ and corresponds to an ionization or refill process to the $s$ lead. The second term is dominant for $\delta\tilde\Omega > T$, where it matches the result at $T = 0$ (opaque junction), see Eq. (20). This process corresponds to an ionization or refill process to the $p$ lead.

The rates for the $\nu = +$ state read

$$\Gamma_+^{\mathrm{I/R}} = \frac{(\mu_B B)^2}{\Delta T} h\left(\frac{\delta\tilde\Omega}{T^2}\right), \tag{24}$$

where

$$h(x) = \frac{1}{\sqrt{2x}} \frac{64x|\sin\phi|}{(8x+\sin^2\phi)^2} \approx \begin{cases} \frac{64}{\sqrt{2}}\sqrt{x}\frac{1}{|\sin\phi|^3}, & \text{for} \quad x \ll 1, \\ \frac{1}{\sqrt{2}}x^{-\frac{3}{2}}|\sin\phi|, & \text{for} \quad x \gg 1. \end{cases} \tag{25}$$

The rates display a narrow peak of height $(\mu_B B)^2/(T\Delta)$ near $\delta\tilde{\Omega} \sim T^2$ and correspond to ionization/refill to the $p$ lead. The coupling to the $s$ lead is negligible in the entire frequency range. At $x \gg 1$, i.e., in the regime $T^2 \ll \delta\tilde{\Omega} \ll 1$, the rates vanish as $T^2(\delta\tilde{\Omega})^{-\frac{3}{2}}$. Thus, in the frequency range of interest for Rabi oscillations, $\Gamma_+^{\rm I} \ll \Gamma_-^{\rm I/R}$.

## V. CURRENT-PHASE RELATION

Being equipped with the occupations of the Andreev levels and the expressions for the field-induced transition rates, obtained in Sec. IV, we calculate the modified current-phase relation in the presence of the magnetic field.

### A. Circular polarization

Let us start with the case of a circularly polarized magnetic field. Taking into account the considerations in Sec. III, we find the following behavior of the current given by Eq. (9) in different phase intervals. For $\phi \in [\pi, 2\pi]$, only ionization processes are possible. Thus, the bound states are always empty, i.e., $\rho_{00} = 1$ and $\rho_{--} = \rho_{++} = \rho_{22} = 0$. As a consequence, the current equals its equilibrium value, $I^{\rm eq} = I_+ + I_-$. On the other hand, in the intervals $[0,\phi_c]$ and $[\pi - \phi_c, \pi]$, the ac field yields a refill process for the state $\nu = -$. Assuming that the rates for parity nonconserving processes due to the environment are much smaller than the field-induced rates, this state is always filled, i.e., $\rho_{--} = 1$ and $\rho_{00} = \rho_{++} = \rho_{22} = 0$. Thus, the current is $I = I_+ - I_-$.

To evaluate the current in the interval $[\phi_c, \pi - \phi_c]$, which includes the phases $\phi_0$ and $\pi - \phi_0$ where Rabi oscillations take place, we insert the stationary occupations, Eqs. (13)–(16), into Eq. (9). We find that the current

$$I = I^\infty + \frac{\Gamma^2}{\Gamma^2 + (2\delta\omega)^2}(I^0 - I^\infty) \tag{26}$$

is the sum of a background term $I^\infty$ and a resonant term, where $\delta\omega = \Omega + \mathrm{sgn}(\sin\phi)\Omega_{\rm R}$. The background term is given as $I^\infty = \sum_{\nu=\pm} I_\nu(\Gamma_\nu^{\rm I} - \Gamma_\nu^{\rm R})/\Gamma_\nu$, and $\Gamma_\pm = \Gamma_\pm^{\rm I} + \Gamma_\pm^{\rm R}$. The current at resonance is given as

$$I^0 = \frac{\Gamma_\Sigma}{\Gamma^2}\left[\Gamma_\Sigma I^\infty + \frac{|\omega_1|^2}{\Gamma_+\Gamma_-}(I_+ - I_-)\sum_{\nu=\pm}\nu\left(\Gamma_\nu^{\rm I} - \Gamma_\nu^{\rm R}\right)\right], \tag{27}$$

where $|\omega_1|^2 = 4(\mu_B B)^2 T^2 |\sin\phi|(1+|\sin\phi|)/(1+T|\sin\phi|)^2$ and $\Gamma_\Sigma = \sum_{\nu=\pm}\Gamma_\nu$, whereas the width of the resonance is determined by

$$\Gamma = \Gamma_\Sigma\sqrt{1 + \frac{|\omega_1|^2}{\Gamma_+\Gamma_-}}. \tag{28}$$

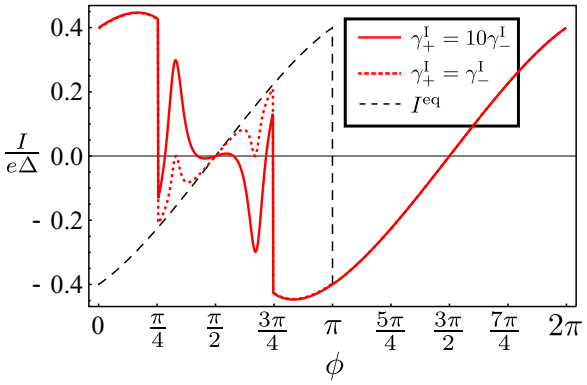


FIG. 4. Current-phase relation for a junction with transmission $T = 0.8$, and a circularly polarized ac magnetic field with amplitude $\mu_B B = 10^{-2}\Delta$ and frequency $\Omega = -1.3\Delta$. The equilibrium current is given for comparison. The current-phase relation is spin sensitive. The phenomenological ionization rates are chosen as $\gamma_+^{\rm I} + \gamma_-^{\rm I} = 10^{-6}\Delta$.

We now assume the two phenomenological rates $\gamma_\nu^{\rm I}$ introduced in Sec. IV A to be nonzero. $I^\infty$ reduces to the equilibrium current, $I^\infty = I^{\rm eq}$. Assuming $\gamma_\pm^{\rm I} \ll |\omega_1|$, the current at resonance is obtained as $I^0 \approx (I_+ - I_-)(\gamma_+^{\rm I} - \gamma_-^{\rm I})/(\gamma_+^{\rm I} + \gamma_-^{\rm I})$, whereas the width of the resonance is $\Gamma \approx |\omega_1|(\gamma_+^{\rm I} + \gamma_-^{\rm I})/\sqrt{\gamma_+^{\rm I}\gamma_-^{\rm I}}$. As the state $\nu = +$ is closer to the continuum, we expect $\gamma_+^{\rm I} \geqslant \gamma_-^{\rm I}$. Depending on their relative magnitude, the current may be completely suppressed at resonance, when $\gamma_-^{\rm I} = \gamma_+^{\rm I}$, or change its sign as compared to the equilibrium current, reaching a magnitude $I^0 \approx I_+ - I_-$, when $\gamma_-^{\rm I} \ll \gamma_+^{\rm I}$.

Figure 4 shows the nonequilibrium current-phase relation for a circularly polarized Zeeman field at $T = 0.8$. The $2\pi$ periodicity is due to the spin-sensitive manipulation of the bound state occupations. If the sign of $\Omega$ was reversed, the current-phase relation would be phase-shifted by $\pi$, i.e., $I(\Omega,\phi) = I(-\Omega,\phi+\pi)$.

In highly transparent junctions, Rabi oscillations should be visible in a fairly wide range of parameters. The conditions are more restrictive in tunnel junctions.

#### *Tunnel junction*

At small transparency, the bound state energies are given by $E_+ \simeq \mathrm{sgn}(\sin\phi)\Delta[1 - (T^2/8)\sin^2\phi]$ and $E_- \simeq \Delta(T/2)\sin\phi$, up to quadratic order in $T$. Thus, the equilibrium current-phase relation takes the form $I^{\rm eq}(\phi) \simeq -T\,\mathrm{sgn}(\sin\phi)(e\Delta/2)\cos\phi$.

Rabi oscillations may be expected in a narrow frequency range $\Delta < |\Omega| < \Omega_{\rm max} = \Delta(1 + T/2 - T^2/8 + \cdots)$. For a given frequency in that range, there is a small separation $\delta\phi \equiv \phi_0 - \phi_c$ between the phase $\phi_0 \simeq \arcsin[(\Omega^2/\Delta^2 - 1)/T]$, where a resonance in the current-phase relation can be expected, and the phase $\phi_c \simeq \arcsin[2(\Omega/\Delta - 1)/T]$, below which refill processes for the state $\nu = -$ are active. Namely,

$$\delta\phi \simeq \begin{cases} (T/4)\sin^2\phi_0/\cos\phi_0, & \Omega_{\rm max} - |\Omega| \gg T^2\Delta, \\ \sqrt{T/2}, & \Omega_{\rm max} - |\Omega| \ll T^2\Delta. \end{cases} \tag{29}$$

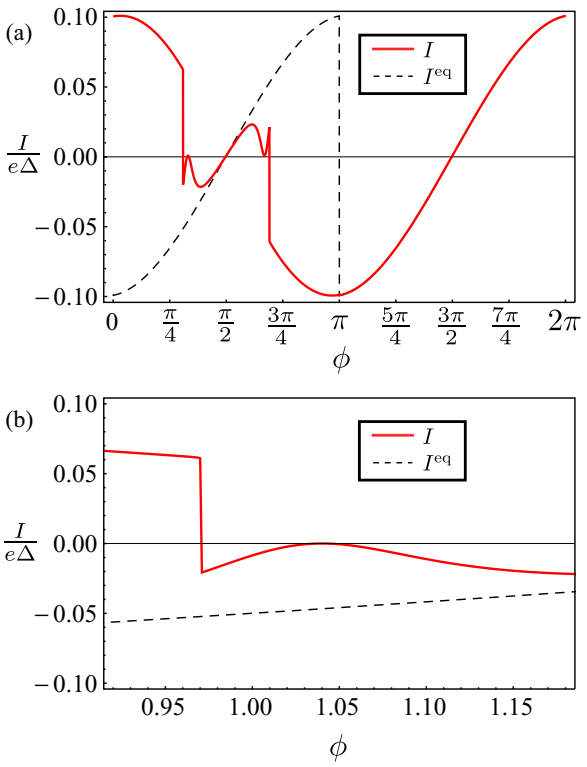


FIG. 5. Current-phase relation for $T = 0.2, \mu_B B = 10^{-2}\Delta, \gamma_+^I + \gamma_-^I = 10^{-6}\Delta$, and $\Omega = -1.08\Delta$ corresponding to $\phi_0 \approx 1.04$. (The frequency has been chosen such that $\phi_0$ is the same as in Fig. 3 for $T = 0.8$.) Panel (b) shows a zoom of panel (a) around the resonance.

Note that in the first case $\delta\phi \ll \pi/2 - \phi_0$ whereas in the second case $\delta\phi \gg \pi/2 - \phi_0$.

The resonance in the current-phase relation remains visible as long as its width is smaller than $\delta\phi$ as well as $\pi/2 - \phi_0$. (Note that, for phases in the intervals $[0,\phi_c]$ and $[\pi - \phi_c, \pi]$, any remnant of Rabi oscillations is completely suppressed as $\Gamma_+^R \ll \Gamma_\pm^I \ll \Gamma_-^R$ drives the system into the odd sector.)

According to Eq. (26), the width of the resonances is given by $\delta\phi_R \sim \Gamma/(T\Delta\cos\phi_0)$. Using the assumption of small phenomenological rates $\gamma$ for a circular polarization, we estimate $\Gamma \propto T\mu_B B$ and, thus, $\delta\phi_R \sim \mu_B B/(\Delta\cos\phi_0)$. When $|\Omega|$ not too close to $\Omega_{\rm max}$, the condition $\delta\phi_R \ll \delta\phi \ll \pi/2 - \phi_0$ yields $\mu_B B \ll T\Delta$. When $\Omega_{\rm max} - |\Omega| \ll T^2\Delta$, on the other hand, the condition $\delta\phi_R \ll \pi/2 - \phi_0 \ll \delta\phi$ yields the more restrictive result $\mu_B B \ll (\Omega_{\rm max} - |\Omega|)/T\Delta \ll T\Delta$. An example is shown in Fig. 5.

### B. Linear polarization

Let us now discuss the case of a linearly polarized field. It follows from Sec. IV A, that under the assumption $\Gamma \ll \Delta$ the steady-state current for a linearly polarized field is given by Eqs. (26)–(28) with $\Gamma_\nu^X = \Gamma_\nu^X(\Omega) + \Gamma_\nu^X(-\Omega)$, where X = I,R.

The current-phase relation for a linearly polarized field is shown in Fig. 6. As the manipulation of the bound state occupations is not spin sensitive, the current is $\pi$ periodic as in equilibrium. Generically, the out-of-equilibrium current-phase relation is $2\pi$ periodic as soon as the ac field carries a finite angular momentum, leading to spin-dependent rates.

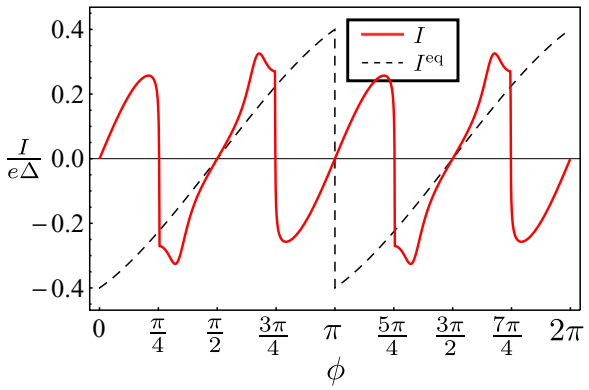


FIG. 6. Current-phase relation for a junction with transmission $T = 0.8$, and a linearly polarized ac magnetic field with amplitude $\mu_B B = 10^{-2}\Delta$ and frequency $\Omega = -1.3\Delta$. The equilibrium current is given for comparison. As in equilibrium, the current-phase relation is $\pi$ periodic. Note that the sign of the current at resonance is reversed as compared to the curves shown in Fig. 4 because $\Gamma_+^I < \Gamma_-^I$.

Let us discuss the relevant rates in more detail. While the refill process of the state $\nu = +$ is energetically not possible in the frequency range, where Rabi oscillations occur, the rate $\Gamma_-^R$ is non zero in the phase intervals $[-\phi_c,\phi_c]$ and $[\pi - \phi_c, \pi + \phi_c]$. The current-phase relation displays a kink at the limit of these intervals; see Fig. 6. The refill rate competes with both ionization rates, which are nonzero for all phase differences. We find $\Gamma_+^I \ll \Gamma_-^I$ in the frequency range of Rabi oscillations. This finding is also illustrated by Figs. 3(a) and 3(b). As a consequence, the width of the resonance in the current-phase relation is determined by the two ionization rates, since we assume that the phenomenological rates are smaller than the field-induced ones. Further, the current at the resonance is approximately $I^0 \approx I_- - I_+$ and has therefore opposite sign with respect to the case of circular polarization.

In the case of a tunnel junction, the finding $\Gamma_+^I \ll \Gamma_-^I$ yields a wide and shallow resonance, which might make its observation difficult.

## VI. CONCLUSIONS

In conclusion, we have shown that the occupations of the Andreev levels in a Josephson junction between an $s$-wave and a $p_x$-wave superconductor can be manipulated using an ac Zeeman field. The induced Rabi oscillations manifest themselves as resonances in the current-phase relation. For a given circular polarization, their presence or absence depends on the spin state of the junction, thus providing a spin detection scheme.

## ACKNOWLEDGMENTS

L.E. thanks Roman-Pascal Riwar for helpful discussions. We acknowledge support by the AGIR program of the Université Grenoble-Alpes, by ANR through Grants No. ANR-11-JS04-003-01 and No. ANR-12-BS04-0016-03, and by an EU-FP7 Marie Curie IRG.

## APPENDIX

In Appendix A, we derive the eigenstates of the Bogoliubov–de Gennes Hamiltonian, Eq. (2). In Appendix B, we use these eigenstates to compute the ionization and refill rates due to an ac Zeeman field, Eq. (17).

## APPENDIX A: Wave functions

In order to obtain the eigenstates of the Hamiltonian (2), we determine the general form of the wave functions in the leads in Sec. A 1. The wave functions are given in the basis $\eta \otimes \tau$, where $\eta$ denotes the R/L space and $\tau$ the particle-hole space. Then we use the boundary condition at the junction to establish the wave functions for the bound states in Sec. A 2, and for the continuum states in Sec. A 3. We provide simple expressions both in the cases of a transparent and an opaque junction. As the wave functions are $2\pi$ periodic, we restrict our considerations to the interval $\phi \in [0, 2\pi[$.

### 1. Wave functions in the leads

In the left ($s$-wave) lead, $x < 0$, the Hamiltonian (2) reduces to

$$\mathcal{H}_\mathrm{s} = v_\mathrm{F} p \eta_z \tau_z - \Delta \tau_x. \tag{A1}$$

It has a block-diagonal structure in the R/L space. In each block, characterized by $\eta_z = \pm 1$, we thus need to solve an auxiliary $2 \times 2$ eigenvalue problem given by

$$(\pm v_\mathrm{F} p \tau_z - \Delta \tau_x) \begin{pmatrix} u \\ v \end{pmatrix} = E \begin{pmatrix} u \\ v \end{pmatrix}. \tag{A2}$$

Using the solutions for this problem, we find that the most general form of the wave functions associated with the Hamiltonian (A1) at energies above the gap, $|E| > \Delta$, is the superposition of four independent spinors,

$$\psi(x) = \frac{1}{\sqrt{1+\alpha^2}} \left[ A_\mathrm{e}^\mathrm{in} \begin{pmatrix} 1 \\ -\alpha \\ 0 \\ 0 \end{pmatrix} e^{ikx} + A_\mathrm{h}^\mathrm{out} \begin{pmatrix} -\alpha \\ 1 \\ 0 \\ 0 \end{pmatrix} e^{-ikx} + A_\mathrm{e}^\mathrm{out} \begin{pmatrix} 0 \\ 0 \\ 1 \\ -\alpha \end{pmatrix} e^{-ikx} + A_\mathrm{h}^\mathrm{in} \begin{pmatrix} 0 \\ 0 \\ -\alpha \\ 1 \end{pmatrix} e^{ikx} \right]. \tag{A3}$$

Here, $\alpha = [E - \mathrm{sgn}(E)\sqrt{E^2 - \Delta^2}]/\Delta$ and $k = \mathrm{sgn}(E)\sqrt{E^2 - \Delta^2}/v_\mathrm{F}$. The prefactor in Eq. (A3) ensures that each four-spinor is normalized to unity. Furthermore,

$$\frac{1}{\sqrt{1+\alpha^2}} = \sqrt{\frac{1}{2}\left(1 + \frac{\sqrt{E^2-\Delta^2}}{|E|}\right)} \quad \text{and} \quad \frac{\alpha}{\sqrt{1+\alpha^2}} = \mathrm{sgn}(E)\sqrt{\frac{1}{2}\left(1 - \frac{\sqrt{E^2-\Delta^2}}{|E|}\right)} \tag{A4}$$

are nothing but the BCS coherence factors. Thus, the spinors with the coefficients $A_\mathrm{e}^\mathrm{in}$, $A_\mathrm{h}^\mathrm{out}$, $A_\mathrm{e}^\mathrm{out}$, and $A_\mathrm{h}^\mathrm{in}$ in Eq. (A3) describe right-moving electron-like, left-moving hole-like, left-moving electron-like, and right moving hole-like quasiparticles, respectively.

Below the gap, $|E| < \Delta$, there are only two evanescent solutions, such that the most general form of the wave functions associated with the Hamiltonian (A1) reads

$$\psi(x) = \left[ B_\mathrm{h} \begin{pmatrix} -\alpha \\ 1 \\ 0 \\ 0 \end{pmatrix} + B_\mathrm{e} \begin{pmatrix} 0 \\ 0 \\ 1 \\ -\alpha \end{pmatrix} \right] e^{\kappa x}. \tag{A5}$$

Here $\alpha = (E - i\sqrt{\Delta^2 - E^2})/\Delta$, which may be written as $\alpha = e^{-i\chi}$, where $\chi \in \mathbb{R}$ is the phase shift acquired in an Andreev reflection process, and $\kappa = \sqrt{\Delta^2 - E^2}/v_\mathrm{F}$ gives the decay length in the lead.

In the right ($p$-wave) lead, $x > L$, the Hamiltonian (2) reduces to

$$\mathcal{H}_\mathrm{p} = v_\mathrm{F} p \eta_z \tau_z - \Delta \eta_z \tau_x e^{-i\tau_z \phi}. \tag{A6}$$

We notice that

$$\mathcal{H}_\mathrm{p} = U^\dagger \mathcal{H}_\mathrm{s} U, \quad \text{where } U = \exp\left[ i\tau_z \left( \frac{\phi}{2} + \frac{\pi}{4}(1+\eta_z) \right) \right]. \tag{A7}$$

This allows us to write the general form of the wave functions both in the continuum,

$$\psi(x) = \frac{1}{\sqrt{1+\alpha^2}} \left[ C_\mathrm{e}^\mathrm{out} \begin{pmatrix} 1 \\ \alpha e^{-i\phi} \\ 0 \\ 0 \end{pmatrix} e^{ikx} + C_\mathrm{h}^\mathrm{in} \begin{pmatrix} \alpha e^{i\phi} \\ 1 \\ 0 \\ 0 \end{pmatrix} e^{-ikx} + C_\mathrm{e}^\mathrm{in} \begin{pmatrix} 0 \\ 0 \\ 1 \\ -\alpha e^{-i\phi} \end{pmatrix} e^{-ikx} + C_\mathrm{h}^\mathrm{out} \begin{pmatrix} 0 \\ 0 \\ -\alpha e^{i\phi} \\ 1 \end{pmatrix} e^{ikx} \right], \tag{A8}$$

and below the gap,

$$\psi(x) = \left[ D_\mathrm{e} \begin{pmatrix} 1 \\ \alpha e^{-i\phi} \\ 0 \\ 0 \end{pmatrix} + D_\mathrm{h} \begin{pmatrix} 0 \\ 0 \\ -\alpha e^{i\phi} \\ 1 \end{pmatrix} \right] e^{-\kappa x}. \tag{A9}$$

To determine the coefficients in the wave functions introduced above, we need to match them at the junction. For this, we derive the transfer matrix $M$ associated with the scalar potential $U(x) = U_0 \theta[x(L-x)]$ in the normal part of the junction. When $U_0$ is large, the wave functions with energy $E$ in the normal part of the junction, $0 < x < L$, are readily obtained as

$$\psi(x) = E_\mathrm{e}^< \begin{pmatrix} 1 \\ 0 \\ -i \\ 0 \end{pmatrix} e^{-\lambda x} + E_\mathrm{e}^> \begin{pmatrix} 1 \\ 0 \\ i \\ 0 \end{pmatrix} e^{\lambda x} + E_\mathrm{h}^< \begin{pmatrix} 0 \\ i \\ 0 \\ 1 \end{pmatrix} e^{-\lambda x} + E_\mathrm{h}^> \begin{pmatrix} 0 \\ -i \\ 0 \\ 1 \end{pmatrix} e^{\lambda x}, \tag{A10}$$

where $\lambda = U_0/v_F$. Using the continuity conditions for the wave functions at $x = 0$ and $x = L$, we can get rid of the coefficients $E_e^<, E_e^>, E_h^<, E_h^>$, and establish the relation

$$\psi(L) = M\psi(0), \tag{A11}$$

where $M = \cosh(\lambda L) + \sinh(\lambda L)\eta_y$. The coefficients in the transfer matrix can be related to the junction transparency, $T = 1/\cosh^2(\lambda L)$. (For definiteness, we will assume $\lambda > 0$ below.) At $T = 0$, the two superconductors are decoupled. In that case, the boundary condition Eq. (A11) reduces to

$$(1 + \eta_y)\psi(0) = 0, \tag{A12}$$

$$(1 - \eta_y)\psi(L) = 0. \tag{A13}$$

Below we use the matching condition (A11) to obtain the bound state and continuum wave functions. Furthermore, we consider the short-junction limit, $L \to 0$, while keeping the product $U_0 L$ that determines the transparency constant.

### 2. Bound state wave functions

In the transparent case, $T = 1$, the matching equation provides two solutions in the R and L sectors, respectively. The solution in the R sector has energy

$$E_R = \Delta \sin\frac{\phi}{2}\,\mathrm{sgn}\,(\sin\phi); \tag{A14}$$

its wave function is obtained with $D_h = B_e = 0$ and $D_e = ie^{i\phi/2}\,\mathrm{sgn}\,(\sin\phi)B_h$. Using the normalization condition for the wave function, we can fix $B_h = \sqrt{\Delta|\cos(\phi/2)|/(2v_F)} = \sqrt{\kappa_R/2}$. The solution in the L sector has energy

$$E_L = \Delta\cos\frac{\phi}{2}; \tag{A15}$$

its wave function is obtained with $D_e = B_h = 0$ and $D_h = -e^{-i\phi/2}B_e$, where $B_e = \sqrt{\Delta|\sin(\phi/2)|/(2v_F)} = \sqrt{\kappa_L/2}$.

The two states cross at $\phi = \pi/2$ and $\phi = 3\pi/2$. The connection to the energy $E_+$ ($E_-$) given in the main text is made by taking for each interval the state with the higher (lower) absolute value of the energy, i.e.,

$$E_+(\phi) = \mathrm{sgn}\,(\sin\phi)\max\{|E_R(\phi)|, |E_L(\phi)|\}, \tag{A16}$$

$$E_-(\phi) = \mathrm{sgn}\,(\sin\phi)\min\{|E_R(\phi)|, |E_L(\phi)|\}. \tag{A17}$$

At finite backscattering, these solutions hybridize and an avoided crossing appears near the phases $\phi = \frac{\pi}{2}$ and $\phi = \frac{3\pi}{2}$. In the opaque case, $T = 0$, the higher-energy state merges with the continuum while the matching equation provides a unique bound state solution with energy $E_- = 0$ that resides on the right side of the junction only. The coefficients are given as $B_h = B_e = 0$ and $D_h = e^{-i\phi}D_e$ with $D_e = \sqrt{\Delta/(2v_F)} = \sqrt{\kappa_-/2}$.

At arbitrary transmission, we find two eigenstates with energies given by Eq. (3). Using the matching condition, Eq. (A11), and the normalization condition, $\int dx|\Psi(x)|^2 = 1$, we obtain the coefficients for the bound state with energy $E_\nu$:

$$B_e^\nu = \sqrt{T}\cos\left(\chi_\nu + \frac{\phi}{2}\right)C^\nu, \tag{A18}$$

$$B_h^\nu = -i\sqrt{T(1-T)}\cos\frac{\phi}{2}C^\nu, \tag{A19}$$

$$D_e^\nu = \sqrt{1-T}e^{i\frac{\phi}{2}}\sin\chi_\nu C^\nu, \tag{A20}$$

$$D_h^\nu = \left[(1-T)\cos\frac{\phi}{2} - e^{-i\chi_\nu}\cos\left(\chi_\nu + \frac{\phi}{2}\right)\right]C^\nu, \tag{A21}$$

where

$$C^\nu = \sqrt{\frac{\kappa_\nu}{2\cos 2\chi_\nu\left(T\cos^2\frac{\phi}{2} - \sin^2\chi_\nu\right)}}. \tag{A22}$$

Note that the expressions previously given for the special cases $T = 0$ and $T = 1$ differ by an irrelevant global phase factor.

### 3. Continuum wave functions

For a fixed energy in the continuum, $|E| > \Delta$, the relation between the four incoming and four outgoing wave functions encoded in Eqs. (A3) and (A8) can be expressed through a scattering matrix $S(E)$ such that

$$\begin{pmatrix} A_e^{in} \\ C_e^{in} \\ A_h^{in} \\ C_h^{in} \end{pmatrix} = S^{-1}(E)\begin{pmatrix} A_e^{out} \\ C_e^{out} \\ A_h^{out} \\ C_h^{out} \end{pmatrix}. \tag{A23}$$

The scattering matrix is unitary, i.e., $S^{-1} = S^\dagger$. At energies $|E| \gg \Delta$, the scattering matrix simplifies to $S = -i\sqrt{1-T}\tau_z + \sqrt{T}\eta_x$, in agreement with the transfer matrix introduced in Eq. (A11).

For a transparent junction, $T = 1$, the scattering matrix is block diagonal as the R and L sectors decouple. It reads

$$S = \begin{pmatrix} 0 & \frac{1-\alpha^2}{1-\alpha^2 e^{i\phi}} & \frac{\alpha(1-e^{i\phi})}{1-\alpha^2 e^{i\phi}} & 0 \\ \frac{1-\alpha^2}{1+\alpha^2 e^{-i\phi}} & 0 & 0 & -\frac{\alpha(1+e^{i\phi})}{1+\alpha^2 e^{-i\phi}} \\ \frac{\alpha(1+e^{-i\phi})}{1+\alpha^2 e^{-i\phi}} & 0 & 0 & \frac{1-\alpha^2}{1+\alpha^2 e^{-i\phi}} \\ 0 & \frac{\alpha(e^{-i\phi}-1)}{1-\alpha^2 e^{i\phi}} & \frac{1-\alpha^2}{1-\alpha^2 e^{i\phi}} & 0 \end{pmatrix}. \tag{A24}$$

For the opaque junction, $T = 0$, scattering states are confined within each lead, and the scattering matrix reads

$$S = \begin{pmatrix} -i & 0 & 0 & 0 \\ 0 & i\frac{\alpha^2-1}{1+\alpha^2} & 0 & -\frac{2\alpha}{1+\alpha^2}e^{i\phi} \\ 0 & 0 & i & 0 \\ 0 & \frac{2\alpha}{1+\alpha^2}e^{-i\phi} & 0 & -i\frac{\alpha^2-1}{1+\alpha^2} \end{pmatrix}$$

$$= \begin{pmatrix} -i & 0 & 0 & 0 \\ 0 & i\sqrt{1-\frac{\Delta^2}{E^2}} & 0 & -\frac{\Delta}{E}e^{i\phi} \\ 0 & 0 & i & 0 \\ 0 & \frac{\Delta}{E}e^{-i\phi} & 0 & -i\sqrt{1-\frac{\Delta^2}{E^2}} \end{pmatrix}, \tag{A25}$$

where we used Eqs. (A4) in the last step.

In the general case, using the matching condition in Eq. (A11) and the continuum wave functions in Eqs. (A3) and (A8), the inverse scattering matrix can be written as $S^{-1} = B^{-1}A$ with

$$A = \begin{pmatrix} 0 & -1 & -\alpha\sqrt{T} & -i\sqrt{1-T}\alpha e^{i\phi} \\ 0 & -\alpha e^{-i\phi} & \sqrt{T} & i\sqrt{1-T} \\ \sqrt{T} & -i\sqrt{1-T} & 0 & \alpha e^{i\phi} \\ -\alpha\sqrt{T} & -i\sqrt{1-T}\alpha e^{-i\phi} & 0 & -1 \end{pmatrix}, \tag{A26}$$

$$B = \begin{pmatrix} -\sqrt{T} & -i\sqrt{1-T} & 0 & \alpha e^{i\phi} \\ \alpha\sqrt{T} & i\alpha\sqrt{1-T}e^{-i\phi} & 0 & 1 \\ 0 & 1 & \alpha\sqrt{T} & i\sqrt{1-T}\alpha e^{i\phi} \\ 0 & -\alpha e^{-i\phi} & -\sqrt{T} & i\sqrt{1-T} \end{pmatrix}. \tag{A27}$$

In the following, we will use the outgoing continuum states. Their wave function is obtained by setting one of the outgoing coefficients $A_e^{out}, C_e^{out}, A_h^{out}, C_h^{out}$ to unity and computing the incoming coefficients via the scattering matrix, Eq. (A23).

## APPENDIX B: TRANSITION RATES

In this section we calculate the ionization and refill rates induced by a weak ac Zeeman field using second-order perturbation theory. For this, we first derive the Hamiltonian due to the Zeeman field, Eq. (8), in the unperturbed basis of the wave functions introduced in Appendix A. Introducing the Bogoliubov transformation,

$$\Psi(x) = \sum_\lambda \psi_\lambda(x)\gamma_\lambda, \tag{B1}$$

inserting it into Eq. (7), and symmetrizing the resulting expression, we obtain

$$H_Z = \frac{\mu_B B}{2} \sum_{\lambda\lambda'} V_{\lambda,\lambda'}\gamma_\lambda\gamma_{\lambda'} + \text{H.c.}, \tag{B2}$$

where $V_{\lambda,\lambda'}$ is given below Eq. (8). Note that $V_{\lambda,\lambda'} = -V_{\lambda',\lambda}$. This allows writing Eq. (B2) as

$$H_Z = \mu_B B e^{-i\Omega t}\left( V_{+,-}\gamma_+\gamma_- + \sum_{E;\mu,\nu} V_{\nu,E\mu}\gamma_\nu\gamma_{E\mu} + \frac{1}{2}\sum_{E,E';\mu,\mu'} V_{E\mu,E'\mu'}\gamma_{E\mu}\gamma_{E'\mu'}\right) + \text{H.c.} \tag{B3}$$

Using the definition of ionization and refill rates, we can calculate them by applying Fermi's golden rule to the Hamiltonian (B3),

$$\Gamma_\nu^{I/R}(\Omega) = 2\pi(\mu_B B)^2 \sum_{E,\mu} |V_{\nu,E\mu}|^2 \delta(\Omega + E_\nu + E)\,\theta(\mp E E_\nu). \tag{B4}$$

Here, the upper sign is for an ionization process, whereas the lower sign is for a refill process. The Heaviside function appears due to the Fermi-Dirac distributions at zero temperature, ensuring that in a refill process the bound state and the continuum state are empty, and in an ionization process the bound state is occupied whereas the continuum state is empty. Noting that $\text{sgn}(E_\nu) = \text{sgn}(\sin\phi)$, we obtain

$$\Gamma_\nu^{I/R}(\Omega) = 2\pi(\mu_B B)^2 \sum_{E'>0,\mu} \left|V_{\nu;\mp E'\,\text{sgn}(\sin\phi),\mu}\right|^2 \times \delta[\Omega + (|E_\nu| \mp E')\,\text{sgn}(\sin\phi)]. \tag{B5}$$

Using the density of states in the leads $\rho(E)$, we can replace the sum by an integral and obtain Eq. (17).

To obtain the matrix elements $V_{\nu,E\mu}$, we use the general expressions for the bound state wave functions and the continuum wave functions, defined above in Eqs. (A5), (A9) and (A3), (A8), respectively. After integration over the real space coordinate and reorganization, we obtain

$$V_{\nu,E\mu} = \frac{1}{\sqrt{1+\alpha^2}}\left(\frac{F_1^\nu}{\kappa_\nu + ik} + \frac{F_2^\nu}{\kappa_\nu - ik}\right), \tag{B6}$$

where

$$F_1^\nu = \left(B_e A_e^{in} - B_h A_h^{in}\right)(\alpha - e^{-i\chi_\nu}) + \left(D_h C_h^{in} e^{i\phi} + D_e C_e^{in} e^{-i\phi}\right)(\alpha + e^{-i\chi_\nu}), \tag{B7}$$

$$F_2^\nu = \left(B_e A_h^{out} - B_h A_e^{out}\right)(\alpha e^{-i\chi_\nu} - 1) + \left(D_h C_e^{out} - D_e C_h^{out}\right)(1 + \alpha e^{-i\chi_\nu}). \tag{B8}$$

Using the outgoing wave functions as defined above, Eq. (B6) can be evaluated numerically to obtain the rates for arbitrary transmission, for an example see Fig. 3. In the following, we consider the two special cases of a transparent and a tunnel junction, for which we give analytical expressions.

### 1. Transparent junction

Here, we want to calculate the rates given by Eq. (17) for $T = 1$. We have seen that there are two bound states, labeled by R and L, with energies given in Eqs. (A14) and (A15). For

each of them, we need to evaluate (B6). Since the calculation is very similar in both cases, we will only show the explicit calculation for $\nu = \mathrm{L}$. Using the coefficients for $T = 1$, given below Eq. (A15), and $\chi_{\mathrm{L}} = \phi/2$, we find

$$V_{\mathrm{L},E\mu} = \sqrt{\frac{\kappa_{\mathrm{L}}}{2(1+\alpha^2)}}\left[\frac{A_{\mathrm{e}}^{\mathrm{in}}\left(\alpha - e^{-i\frac{\phi}{2}}\right) - C_{\mathrm{h}}^{\mathrm{in}}\left(\alpha e^{i\frac{\phi}{2}} + 1\right)}{\kappa_{\mathrm{L}} + ik} + \frac{A_{\mathrm{h}}^{\mathrm{out}}\left(\alpha e^{-i\frac{\phi}{2}} - 1\right) - e^{-i\frac{\phi}{2}} C_{\mathrm{e}}^{\mathrm{out}}\left(1 + \alpha e^{-i\frac{\phi}{2}}\right)}{\kappa_{\mathrm{L}} - ik}\right]. \tag{B9}$$

For the transparent junction, there are only two outgoing states, $C_{\mathrm{e}}^{\mathrm{out}} = 1$ or $A_{\mathrm{h}}^{\mathrm{out}} = 1$. Then,

$$\begin{aligned}\sum_{\mu}\left|V_{\mathrm{L},E\mu}\right|^2 = \frac{\kappa_{\mathrm{L}}}{2(1+\alpha^2)}\Bigg\{&\frac{2(1+\alpha^2)}{\kappa_{\mathrm{L}}^2+k^2} + \frac{\alpha^2 - 2\alpha\epsilon_{\mathrm{L}} + 1}{\kappa_{\mathrm{L}}^2+k^2}\left(|S_{21}|^2 + |S_{31}|^2\right) + \frac{\alpha^2 + 2\alpha\epsilon_{\mathrm{L}} + 1}{\kappa_{\mathrm{L}}^2+k^2}\left(|S_{24}|^2 + |S_{34}|^2\right) \\ &- \frac{2}{\kappa_{\mathrm{L}}^2+k^2}\,\mathrm{Re}\left[\left(\alpha - e^{-i\frac{\phi}{2}}\right)\left(1 + \alpha e^{-i\frac{\phi}{2}}\right)\left(S_{21}^* S_{24} + S_{31}^* S_{34}\right)\right] + 2\,\mathrm{Re}\left[\frac{1}{(\kappa_{\mathrm{L}} + ik)^2} H_1\right] + 2\,\mathrm{Re}\left[\frac{1}{(\kappa_{\mathrm{L}} - ik)^2} H_2\right]\Bigg\},\end{aligned} \tag{B10}$$

where

$$H_1 = \left(\alpha - e^{-i\frac{\phi}{2}}\right)\left[-S_{21}^*\left(\alpha e^{-i\phi} + e^{i\frac{\phi}{2}}\right) + S_{31}^*\left(-1 + \alpha e^{i\frac{\phi}{2}}\right)\right], \tag{B11}$$

$$H_2 = -\left(1 + \alpha e^{-i\frac{\phi}{2}}\right)\left[-S_{24}\left(\alpha e^{-i\phi} + e^{-i\frac{\phi}{2}}\right) + S_{34}\left(-1 + \alpha e^{-i\frac{\phi}{2}}\right)\right]. \tag{B12}$$

Using the unitarity of the scattering matrix, $\sum_k S_{ik} S_{jk}^* = \delta_{ij}$, we find

$$\sum_{\mu}\left|V_{\mathrm{L},E\mu}\right|^2 = \frac{2\kappa_{\mathrm{L}}}{\kappa_{\mathrm{L}}^2+k^2} + \frac{\kappa_{\mathrm{L}}}{1+\alpha^2}\left(\frac{\kappa_{\mathrm{L}}^2 - k^2}{\left(\kappa_{\mathrm{L}}^2+k^2\right)^2}\,\mathrm{Re}\left[H_1 + H_2\right] + \frac{2\kappa_{\mathrm{L}} k}{\left(\kappa_{\mathrm{L}}^2+k^2\right)^2}\,\mathrm{Im}\left[H_1 - H_2\right]\right), \tag{B13}$$

which, after lengthy but straightforward algebraic manipulation, yields

$$\begin{aligned}\sum_{\mu}\left|V_{\mathrm{L},E\mu}\right|^2 &= \frac{2\kappa_{\mathrm{L}}}{\kappa_{\mathrm{L}}^2+k^2}\left[1 + \frac{\kappa_{\mathrm{L}}^2 - k^2}{\kappa_{\mathrm{L}}^2+k^2}\,\frac{1 - 4\alpha^2 + \alpha^4 - 2\alpha^2\cos\phi}{1 + \alpha^4 + 2\alpha^2\cos\phi} + \frac{\kappa_{\mathrm{L}} k}{\kappa_{\mathrm{L}}^2+k^2}\,\frac{8\alpha^2(\alpha^2-1)\sin\phi}{(1+\alpha^2)(1+\alpha^4+2\alpha^2\cos\phi)}\right]. \\ &= \frac{v_{\mathrm{F}}}{\Delta}\,\frac{4\left|\sin\frac{\phi}{2}\right|(\epsilon^2-1)}{\left(\epsilon^2 - \cos^2\frac{\phi}{2}\right)^2\left(\epsilon^2 - \sin^2\frac{\phi}{2}\right)}\left[1 - \frac{\sin\phi\,|\sin\frac{\phi}{2}|}{\epsilon}\right],\end{aligned} \tag{B14}$$

where $\epsilon = E/\Delta$. Repeating the calculation for $\nu = \mathrm{R}$ and using the expressions for the bound state energies, Eqs. (A14) and (A15), we finally obtain

$$\sum_{\eta}\left|V_{\nu,\eta}\right|^2 = \frac{v_{\mathrm{F}}}{\Delta}\,\frac{4|\epsilon_{\bar{\nu}}|(\epsilon^2-1)}{(\epsilon^2 - \epsilon_{\nu}^2)^2(\epsilon^2 - \epsilon_{\bar{\nu}}^2)}\left[1 - \frac{\sin\phi|\epsilon_{\bar{\nu}}|}{\epsilon}\right], \tag{B15}$$

where $\epsilon_\nu = E_\nu/\Delta$ and $\bar{\mathrm{R}} = \mathrm{L}$ and $\bar{\mathrm{L}} = \mathrm{R}$. Substituting (B15) into (B5) and using the energy conservation condition, $|\epsilon| = |\tilde{\Omega}| + |\epsilon_\nu|$ for an ionization process and $|\epsilon| = |\tilde{\Omega}| - |\epsilon_\nu|$ for a refill process, we find the rates given in Eq. (18).

### 2. Opaque junction

We evaluate (B6) for the opaque junction, $T = 0$, where only the bound state $\nu = -$ exists. Using the coefficients derived in Sec. A 2, we obtain

$$\begin{aligned}V_{-,E\mu} = e^{-i\phi}\sqrt{\frac{\kappa_-}{2(1+\alpha^2)}}\Bigg[&-i\,\frac{C_{\mathrm{h}}^{\mathrm{in}} e^{i\phi} + C_{\mathrm{e}}^{\mathrm{in}}}{\kappa_- + ik}(1 + i\alpha) \\ &+ \frac{C_{\mathrm{e}}^{\mathrm{out}} - C_{\mathrm{h}}^{\mathrm{out}} e^{i\phi}}{\kappa_- - ik}(1 - i\alpha)\Bigg].\end{aligned} \tag{B16}$$

As in the transparent case, there are only two outgoing states, $C_{\mathrm{e}}^{\mathrm{out}} = 1$ or $C_{\mathrm{h}}^{\mathrm{out}} = 1$. After some algebra and using the unitarity of the scattering matrix, we find

$$\begin{aligned}\sum_{\mu}\left|V_{-,E\mu}\right|^2 = \frac{\kappa_-}{1+\alpha^2}\Bigg\{&2\,\frac{1+\alpha^2}{\kappa_-^2+k^2} \\ &- \mathrm{Im}\left[\frac{(1-i\alpha)^2}{(\kappa_- - ik)^2}\left(S_{22} - S_{24} + e^{-i\phi}S_{44} - e^{i\phi}S_{42}\right)\right]\Bigg\}.\end{aligned} \tag{B17}$$

Using the scattering matrix (A25), we finally obtain

$$\sum_{\mu}\left|V_{-,E\mu}\right|^2 = \frac{v_{\mathrm{F}}}{\Delta}\,\frac{16(\epsilon^2-1)}{\epsilon^6}. \tag{B18}$$

The corresponding rate is given in Eq. (20).

[1] H.-J. Kwon, K. Sengupta, and V. Yakovenko, Eur. Phys. J. B **37**, 349 (2004).
[2] Y. Asano, Phys. Rev. B **64**, 224515 (2001).
[3] N. Yoshida, Y. Tanaka, S. Kashiwaya, and J. Inoue, J. Low Temp. Phys. **117**, 563 (1999).
[4] Y. Asano and S. Yamano, Phys. Rev. B **84**, 064526 (2011).
[5] P. Burset, F. Keidel, Y. Tanaka, N. Nagaosa, and B. Trauzettel, Phys. Rev. B **90**, 085438 (2014).
[6] C.-K. Lu and S. Yip, Phys. Rev. B **80**, 024504 (2009).
[7] S. B. Chung, J. Horowitz, and X.-L. Qi, Phys. Rev. B **88**, 214514 (2013).
[8] K. Sengupta and V. M. Yakovenko, Phys. Rev. Lett. **101**, 187003 (2008).
[9] Z. H. Yang, J. Wang, and K. S. Chan, J. Phys. Condens. Matter **23**, 085701 (2011).
[10] S. Yip, J. Low Temp. Phys. **91**, 203 (1993).
[11] Y. Asano, Y. Tanaka, M. Sigrist, and S. Kashiwaya, Phys. Rev. B **67**, 184505 (2003).
[12] J. Michelsen, V. S. Shumeiko, and G. Wendin, Phys. Rev. B **77**, 184506 (2008).
[13] F. S. Bergeret, P. Virtanen, T. T. Heikkilä, and J. C. Cuevas, Phys. Rev. Lett. **105**, 117001 (2010).
[14] F. S. Bergeret, P. Virtanen, A. Ozaeta, T. T. Heikkilä, and J. C. Cuevas, Phys. Rev. B **84**, 054504 (2011).
[15] S. Teber, C. Holmqvist, and M. Fogelström, Phys. Rev. B **81**, 174503 (2010).
[16] D. Jerome, A. Mazaud, M. Ribault, and K. Bechgaard, J. Phys. Lett. **41**, 95 (1980).
[17] V. P. Mineev and K. V. Samokhin, *Introduction to Unconventional Superconductivity* (Gordon and Breach, Amsterdam, 1999).
[18] A. Y. Kitaev, Phys. Usp. **44**, 131 (2001).
[19] D. G. Olivares, A. L. Yeyati, L. Bretheau, Ç. Ö. Girit, H. Pothier, and C. Urbina, Phys. Rev. B **89**, 104504 (2014).
[20] R.-P. Riwar, M. Houzet, J. S. Meyer, and Y. V. Nazarov, J. Phys. Condens. Matter **27**, 095701 (2015).